

Superconductivity of bipolarons from quadratic electron-phonon interaction

Zhongjin Zhang,¹ Anatoly Kuklov,² Nikolay Prokof'ev,¹ and Boris Svistunov¹

¹*Department of Physics, University of Massachusetts, Amherst, MA 01003, USA*

²*Department of Physics & Astronomy, College of Staten Island and the Graduate Center of CUNY, Staten Island, NY 10314*

In systems with linear electron-phonon interaction (EPI), bound states of polarons, or bipolarons, form by gaining energy from the lattice deformation. The quadratic EPI case is fundamentally different: bipolarons form because electrons lose less energy when the total charge density is “compactified.” As the coupling constant is increased, the bipolarons first appear as extended (but finite radius) soliton-type states. They subsequently decrease in radius until their size reaches the inter-atomic scale. We present the first numerically exact solution of the bipolaron problem from quadratic EPI in the presence of both on-site Hubbard and long-range Coulomb repulsion, and compute estimates of the largest superconducting transition temperature within the bipolaron mechanism. We find that T_c/Ω ratios, where Ω is the optical phonon frequency, can be several times larger than what one may expect from the linear EPI provided the phonon frequency is increased by orders of magnitude on occupied sites. Electron-electron repulsion can be tolerated at the expense of stronger EPI and the most detrimental effect comes from the Coulomb potential because it easily eliminates extended soliton states.

When electrons couple to lattice vibrations their low-energy properties such as the dispersion, $\epsilon(\mathbf{k})$, effective mass, m_* , and residue, Z , get renormalized; the resulting quasiparticle is called a polaron [1]. In the strong coupling limit, the electron-phonon interaction (EPI) can also cause two polarons to form a bound state of size R , or a bipolaron. At finite but low enough density, when bipolarons can be treated as point bosons with repulsive effective interaction, the transition temperature to the superconducting state can be accurately estimated from (see Ref. [2])

$$T_c(n_b) \approx 3.31n_b^{2/3}/m_*. \quad (1)$$

The maximum value of T_c within the bipolaron mechanism follows from the “marginal overlap” condition on the bipolaron density n_b , namely $4\pi R^3 n_b = 1$. On a lattice, this condition makes sense only if $R > a$ where a is the lattice constant. When two electrons form a bound state localized on a single site, one formally has $R \ll a$ but the density is still limited because bipolarons cannot occupy the same site. To reflect this fact, we introduce effective radius squared, $R_*^2 = \max(R^2, a^2)$, and use it instead of R^2 in the no-overlap condition. This leads to the following estimate for the largest transition temperature [2]

$$T_c \sim \frac{1.3}{m_* R_*^2}, \quad (2)$$

in terms of single bipolaron parameters. This estimate clearly shows that high values of T_c require light and compact bipolarons.

Nearly all work on bipolarons in the past was limited to linear (in terms of atomic displacements) EPI when bound states form by gaining energy from large lattice distortion. In the most relevant for materials adiabatic limit $\Omega/W \ll 1$, where Ω is the characteristic phonon frequency and W is the bare electron bandwidth, this inter-

action mechanism leads either to exponentially heavy (interatomic size) bipolarons or large-radius shallow states with sharp crossover between the two [3, 4]. Systems with phonon-assisted hopping EPI have larger T_c/Ω ratios than systems with density-displacement EPI, but in all known cases, this ratio remains much smaller than unity [4, 5] in the adiabatic limit.

This outcome motivates one to consider alternative mechanisms of EPI, and one promising example is quadratic density-displacement coupling

$$H_{\text{ep}} = g_2 \sum_i n_i \frac{M\Omega^2 x_i^2}{2} \equiv g_2 \frac{\Omega}{4} \sum_i n_i (b_i + b_i^\dagger)^2, \quad (3)$$

which results in light compact polarons [6, 7]. Here b_i is the bosonic annihilation operator on site i , n_i is the electron occupation number, $n_i = \sum_\sigma n_{i\sigma}$, and $g_2 > 0$ is the dimensionless coupling constant. The effects of weak quadratic coupling to phonons in the Fermi liquid regime was considered numerous times in the past [8–26]. The soliton-type polaron [6, 7, 27–30] and bipolaron [31] formation within the variational approach in continuum was addressed too, and it has been realized that the effective mass is not exponentially suppressed at strong coupling. However, so far the entire strong coupling regime for bipolarons and optimal T_c values have not been solved. Recently, a special case—the atomic limit (AL) in the absence of interelectron repulsion was investigated in Ref. [32]. [The AL regime corresponds to large values of g_2 when both electrons reside on one and the same lattice site.] The most important result of this study is that, similarly to single polarons [6, 7], the bipolaron mass in this extreme limit remains moderately enhanced and weakly dependent on the coupling constant. However, the physics of extended soliton states, which form well before the AL is reached, suggests that optimal values of T_c are expected for soliton states before they collapse to the AL because compact solitons are

light and their masses are nearly independent of g_2 (or even decrease with increasing coupling [7]).

The non-interacting part of the Hamiltonian considered in this work describes electrons with nearest neighbor hopping on the simple cubic lattice and dispersionless optical phonons (we count energy from the ground state of non-interacting harmonic oscillators):

$$H_0 = -t \sum_{\langle ij \rangle, \sigma} c_{j\sigma}^\dagger c_{i\sigma} + \Omega \sum_i b_i^\dagger b_i. \quad (4)$$

Here $c_{i\sigma}^\dagger$ ($c_{i\sigma}$) create (annihilate) electron with spin σ on site i . The value of t is chosen as the unit of energy, and the lattice constant a as the unit of length. Apart from EPI (3) the interacting Hamiltonian also includes direct electron-electron repulsion characterized by the on-site Hubbard term U and long-range Coulomb potential $V(r > 0) = V(a/r)$:

$$H_{ee} = U \sum_i n_{i\uparrow} n_{i\downarrow} + \sum_{i \neq j} V(|r_i - r_j|) n_{i\uparrow} n_{j\downarrow}. \quad (5)$$

According to Hamiltonian (3), the phonon frequency on sites with the occupation number n is changed to

$$\tilde{\Omega}_n = \Omega r_n, \quad r_n = \sqrt{1 + g_2 n}. \quad (6)$$

If g_2 is negative (the model is stable only at $g_2 \geq -1/2$) the energy gain due to change in the harmonic oscillator zero-point energy on doubly occupied site is larger than that on two distant singly occupied sites

$$U_{\text{eff}} = \frac{\Omega}{2} [r_2 - 1 - 2(r_1 - 1)] = \frac{\Omega}{2} [r_2 + 1 - 2r_1] \leq 0. \quad (7)$$

In the adiabatic limit, this weak attraction (even in the absence of Hubbard and Coulomb repulsion) cannot bind electrons in three dimensions. However, U_{eff} is negative also for positive g_2 because energy increase with electron density is sub-linear. This is the prime reason why polarons at strong coupling form extended self-trapped soliton states [7, 27–29, 31]. It is then expected that bipolarons first appear as extended finite-radius solitons; the radius decreasing with g_2 until the AL is reached at approximately $U + U_{\text{eff}} < -W/2$ (in the simple cubic lattice $W = 12t$), i.e. at

$$g_{\text{AL}} \sim 3 \left(\frac{W + 2U}{\Omega} \right)^2. \quad (8)$$

In this work, we first look into the atomic limit $g_2 > g_{\text{AL}}$, add the effects of electron-electron interaction to the theoretical description, and use it as a benchmark for numerical simulations of the effective mass, the bound state size, and T_c estimates in this limit. We perform numeric simulations of the system Hamiltonian in the basis of atomic coordinates using the X -representation Monte Carlo technique (XMC)—a numerically exact sign-free

approach [6, 7, 33]. We obtain accurate results for bipolarons in the entire strong coupling regime for three representative cases (with and without on-site and/or Coulomb interaction) in the realistic adiabatic regime $\Omega/t = 0.1$ or $\Omega/W = 1/120$. We find that the optimal values of T_c/Ω ratio exceed the largest known results based on the linear EPI by several times, and are found on approach to the AL as a result of competition between the shrinking soliton size and increasing mass. The main result is presented in Fig. 1.

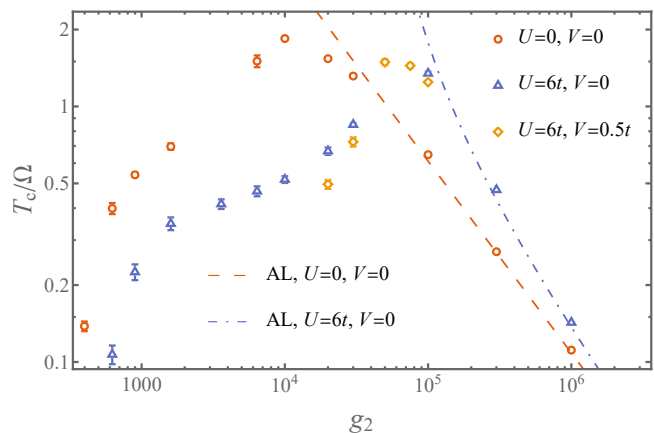


FIG. 1. The critical temperature to phonon frequency ratio as a function of the coupling strength g_2 with and without on-site and/or Coulomb repulsion. Dashed lines are asymptotic predictions for the atomic limit. Bound states disappear for g_2 smaller than the leftmost point for each case, see Fig. 2.

Method. The XMC method is based on the lattice path integral for the electrons and coordinate representation for harmonic oscillators [6, 7, 33]. On the one hand, lattice path-integral allows us to deal with arbitrary interaction potential between the electron because H_{ee} is diagonal in this basis and is kept in the exponent. On the other hand, in the coordinate representation of harmonic oscillators, all EPI effects are absorbed into the harmonic oscillator propagator with the electron occupation number dependent frequency (6). All relevant bipolaron properties are extracted from the electron pair propagator in imaginary time

$$G(\tau, \mathbf{r}_1, \mathbf{r}_2) = \langle \text{vac} | c_{\mathbf{r}_1\uparrow} c_{\mathbf{r}_2\downarrow} e^{-\tau H} c_{\mathbf{0}\downarrow}^\dagger c_{\mathbf{0}\uparrow}^\dagger | \text{vac} \rangle. \quad (9)$$

simulated using Monte Carlo sampling methods. From asymptotic exponential decay of $G_p(\tau)$, which is the Fourier transform of the center-of-mass propagator $G(\tau, \mathbf{R}) = \sum_{\mathbf{r}_1} \sum_{\mathbf{r}_2} \delta_{\mathbf{R}, (\mathbf{r}_1 + \mathbf{r}_2)/2} G(\tau, \mathbf{r}_1, \mathbf{r}_2)$, as a function of imaginary time, we extract the bipolaron energies in different momentum sectors: $G_p(\tau \rightarrow \infty) \sim Z_p e^{-E_p \tau}$. This gives us direct access to the ground-state energy, $E = E_{p=0}$; the effective mass, $1/m_* = d^2 E_p / dp^2$, is extracted by fitting the low-momentum data. Other observables in the ground state are measured in the middle

of the path [4] using asymptotically exact in the $\tau \rightarrow \infty$ limit relation

$$\langle G | \hat{O} | G \rangle = \frac{\langle \text{vac} | c_{\mathbf{r}_1 \uparrow} c_{\mathbf{r}_2 \downarrow} e^{-\tau H/2} \hat{O} e^{-\tau H/2} c_{\mathbf{0} \downarrow}^\dagger c_{\mathbf{0} \uparrow}^\dagger | \text{vac} \rangle}{\langle \text{vac} | c_{\mathbf{r}_1 \uparrow} c_{\mathbf{r}_2 \downarrow} e^{-\tau H} c_{\mathbf{0} \downarrow}^\dagger c_{\mathbf{0} \uparrow}^\dagger | \text{vac} \rangle}. \quad (10)$$

For the operators which are diagonal in the chosen representation, such as electron positions, the computation of (10) is simple: all one needs to do is to collect statistics of the matrix elements $O(\mathbf{r}_1, \mathbf{r}_2)$ of the operator \hat{O} in the coordinate representation. The only minor setup requirement is that the overlap between the initial and ground states, $\langle G | c_{\mathbf{0} \downarrow}^\dagger c_{\mathbf{0} \uparrow}^\dagger | \text{vac} \rangle$, is not too small to produce reliable XMC statistics for propagator (9) at large τ .

All simulations in this work were performed in the realistic adiabatic limit with $\Omega/t = 0.1$. We considered three representative cases: $(U, V) = (0, 0)$, $(6t, 0)$, and $(6t, 0.5t)$; and performed broad scans in terms of the coupling constant g_2 . Apart from the bipolaron effective masses and ground state energies (to determine binding energies, $\Delta E = E - 2E_p$, we had to simulate single-polaron ground state energies E_p as well), we have computed probabilities, $P(\mathbf{r})$, of finding two electrons at a given distance \mathbf{r} from each other, which was subsequently used to obtain the mean square bipolaron radius

$$R^2 = \langle r^2 \rangle = \sum_{\mathbf{r}} r^2 P(\mathbf{r}). \quad (11)$$

Atomic Limit. We first look at the limiting case $g_2 \gg g_{\text{AL}}$ considered in Ref. [32] when the binding state is localized on a single site and generalize the theory to include effects of on-site and Coulomb repulsion. Even for modest adiabatic ratio $\Omega/t = 0.1$ considered in this work, the AL corresponds to very large values of the coupling constant g_2 between 10^4 and 10^5 depending on U [see Eq. (8) and the comparison with the numerically exact solutions below]. When two electrons occupy the same site their energy is $E_{\ell 1} = (\tilde{\Omega}_2 - \Omega)/2 + U = \Omega(r_2 - 1)/2 + U$. If electrons occupy different sites a distance r apart, their energy is $E_{\ell 2}(r) = \tilde{\Omega}_1 - \Omega + V(r) = \Omega(r_1 - 1) + V(r)$. In the AL, the leading binding energy term is then given by the difference between the energies of two localized solutions with $r \rightarrow \infty$

$$\Delta E_\ell = E_{\ell 1} - E_{\ell 2}(r \rightarrow \infty) = U + \frac{\Omega}{2}[r_2 + 1 - 2r_1]. \quad (12)$$

The motion and zero-point fluctuations of tightly bound electrons are through second-order in t processes when in virtual states one finds two electrons on the nearest-neighbor sites with excited oscillator modes. The final result for the effective bipolaron hopping amplitude, t_{eff} , and zero-point fluctuation energy, δE , is a straightforward generalization of calculation done in Ref. [32]

$$t_{\text{eff}} = \frac{2\eta t^2}{\Delta} \int_0^{+\infty} \frac{e^{-z} dz}{1 - \gamma_0 \gamma_2 e^{-2\xi z}}, \quad (13)$$

$$\delta E = -\frac{12\eta t^2}{\Delta} \int_0^{+\infty} \frac{e^{-z} dz}{\sqrt{1 - \gamma_0^2 e^{-2\xi z}} \sqrt{1 - \gamma_2^2 e^{-2\xi z}}}, \quad (14)$$

were

$$\Delta = \Omega[2r_1 - r_2 - 1]/2 - U + V,$$

$$\eta = \frac{4\sqrt{r_2} r_1}{(r_1 + 1)(r_2 + r_1)}, \quad \gamma_m = \frac{r_1 - r_m}{r_1 + r_m},$$

and $\xi = r_1 \Omega / \Delta$ (here we correct the typing mistake in Ref. [32]). With hopping corrections included, the bipolaron binding energy is given by

$$\delta E = \Delta E_\ell + \delta E - 6t_{\text{eff}} + \frac{24\sqrt{r_1} t}{1 + r_1}, \quad (15)$$

where the last term is the kinetic energy gain for two mobile polarons. The effective mass renormalization is simply $m_*/m = t/t_{\text{eff}}$.

Finally, for direct comparison with numerical simulations we present the AL prediction for the bound state radius defined by Eq. (11):

$$\left(\frac{R}{a}\right)^2 = \frac{12\eta t^2}{\Delta^2} \int_0^{+\infty} z e^{-z} dz \left[\frac{1}{1 - \gamma_0 \gamma_2 e^{-2\xi z}} + \frac{1}{\sqrt{1 - \gamma_0^2 e^{-2\xi z}} \sqrt{1 - \gamma_2^2 e^{-2\xi z}}} \right]. \quad (16)$$

It has no effect on T_c estimate based on $R_*^2 = \max(R^2, a^2)$ because in this limit, $R \ll a$, and, thus, the transition temperature is decreasing with increasing g_2 as $1/m_*$. In the asymptotic $g_2 \rightarrow \infty$ limit, we have $E \simeq E_{\ell 1} - 180g_2^{-3/4} t^2 / \Omega$, $m_*/m \simeq 0.076g_2^{3/4} \Omega/t$, and $(R/a)^2 \simeq 550g_2^{-5/4} t^2 / \Omega^2$.

Quantum Solution. Accurate solutions using XMC method can be obtained for any value of g_2 . In all cases considered, for $g_2 > g_{\text{AL}}$ we observe perfect agreement with theoretical predictions for AL, see Figs. 2–4. For realistic $\Omega/t = 0.1$ ratio, this regime corresponds to extremely large coupling $g_2 > 10^5$. For $U = 0$, $V = 0$, the bipolaron state emerges at around $g_2 \approx 400$ with large but finite $R^2 \approx 40$, see Figs. 2 and 3. Simulations at smaller g_2 yield energies E that are slightly larger than the energy of two single polarons $2E_p$ and gradually decreasing with increasing the projection time τ in Eqs. (9) and (10). Concurrently, the measured mean-square radius is diverging with τ . These are clear signatures that the two-particle ground state is unbounded. Large radius bipolaron (and polaron) solitons form because they optimize the trade-off between the smaller positive interaction energy and larger localization energy for high electron density [7, 27, 28, 31]. The value of T_c in this regime is small because of large R_*^2 (large-radius solitons remain relatively light when they form). For larger values of g_2 solitons are getting smaller until they reach the

AL. For T_c this effect is more important than the slow increase of the effective mass, especially given that on the approach to the atomic limit the m_* vs g_2 dependence exhibits a broad plateau (for a smaller adiabatic ratio it is even expected to go through a minimum [7]), see Fig. 4. The broad maximum in T_c is reached for $R^2 \gtrsim 1$ because at stronger coupling the effective mass increase becomes the dominant effect in suppressing the transition temperature. At the maximum the T_c/Ω ratio is as large as 2 and by far exceeds all known best case scenarios for the linear EPI. However, one may not miss the fact that this corresponds to very large values of g_2 when Ω_2 is comparable to the bare electron bandwidth.

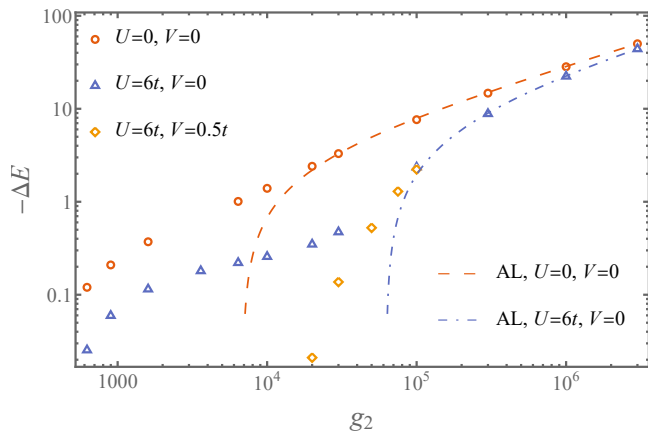


FIG. 2. Bipolaron binding energies as functions of g_2 (data points). Dashed and dashed-dotted lines are the results of AL, Eq. (15). Statistical error bars are much smaller than symbol sizes.

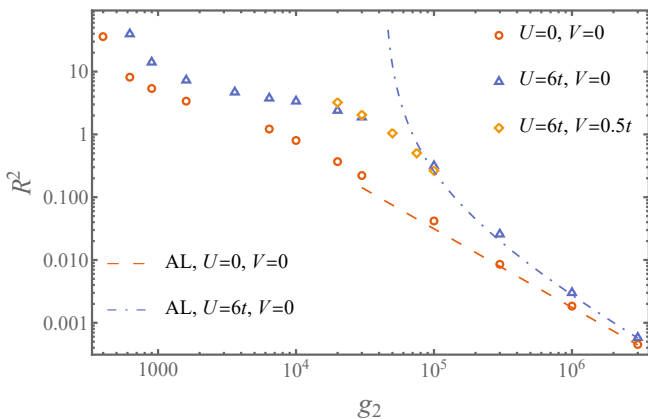


FIG. 3. Bipolaron radii as functions of g_2 (data points). Dashed and dashed-dotted lines are the AL results, Eq. (16). Statistical error bars are much smaller than symbol sizes.

Since the bound state first emerges as a large-radius soliton state, it can easily tolerate strong Hubbard repulsion by developing local inter-particle correlations. As a

result, for $(U/t, V/t) = (6, 0)$ the bipolaron state emerges at slightly larger $g_2 \approx 600$. The most important effect of onsite repulsion is significant shift towards large g_2 for the onset of AL and the development of a broad plateau in both $R^2(g_2)$ and $m_*(g_2)/m$, see Figs. 3 and (4). The maximum of T_c is found at the end of this plateau (see in Fig. 1).

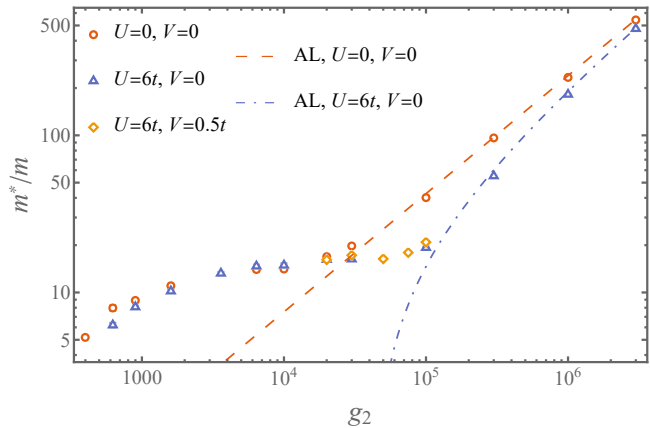


FIG. 4. Effective masses as functions of g_2 (data points). Dashed and dashed-dotted lines are the results of AL when $m_*/m = t/t_{\text{eff}}$, see Eq. (13). Error bars are shown but are typically smaller than symbol sizes.

On the one hand, while remaining stable against Hubbard U large bipolarons most likely form an attractive Bose gas, i.e. the system is unstable against phase separation. On the other hand, compact bipolarons (certainly in the AL) repel each other because of the Pauli principle [32]. The phase separation scenario is eliminated by adding Coulomb repulsion, but our simulations show that even relatively weak Coulomb potential with $V/t = 0.5$ shifts the threshold for bipolaron formation by orders of magnitude! Now bipolarons first emerge at $g_2 \approx 2 \times 10^4$ as small size, $(R/a)^2 \sim 3$, states. However, their properties and subsequent evolution towards AL is nearly independent of V , see Figs. 1-4. This outcome ensures that in the region of T_c maximum bipolarons form a stable superconducting state.

Conclusions. We present numerically exact results for bipolarons from quadratic EPI with and without the electron-electron interaction in the adiabatic regime with $\Omega/t = 0.1$. Our data cover the entire strong coupling regime from the threshold of forming a shallow large-radius soliton state to its evolution towards compact bipolarons, and, ultimately, to the atomic limit when electrons are tightly bound on a single site. The effective masses of bipolarons remain relatively light and exhibit extremely weak dependence on the EPI until the atomic limit is reached. This leads to a maximum of T_c estimated from Eq. (2) on approach to the atomic limit when $(R/a)^2 \gtrsim 1$. At the maximum the T_c/Ω ratio is

much larger than what is possible to achieve in all known models with the linear EPI, but the quadratic coupling must be such that the locally renormalized phonon frequency be comparable to the bare electron bandwidth. Realistically, this situation may describe quadratic EPI to a soft (or near critical) mode, $\Omega \rightarrow 0$ at $g_2\Omega^2 = \text{const}$. This outcome also suggests that high- T_c mechanism is easier to get for larger Ω/t ratios. The XMC method used to solve the problem, can be generalized to models with arbitrary density-displacement coupling, arbitrary sign-positive displacement dependent hopping $t(x)$, and dispersive phonons [33] to investigate whether even higher values of T_c are feasible within the bipolaron mechanism of superconductivity.

The essence of the binding mechanism discussed here is minimization of the phonon zero-point energy. It turns out that thermal fluctuations *increase* the free energy balance in favor of bipolarons and the thermal contribution becomes dominant at $T > \Omega\sqrt{g_2}/\ln(g_2)$, i.e. at temperature much lower than the ground-state binding energy. This motivates further studies of finite- T effects; in particular, the extent of the preformed pairs regime.

AK, NP and BS acknowledge support from the National Science Foundation under Grants DMR-2335905 and DMR-2335904, ZZ acknowledges support from the Simons collaboration on new frontiers in superconductivity. This work was performed in part at Aspen Center for Physics, which is supported by National Science Foundation grant PHY-2210452.

-
- [1] L. Landau, Electron motion in crystal lattices, Phys. Z. Sowjetunion **3**, 664 (1933).
- [2] C. Zhang, B. Capogrosso-Sansone, M. Boninsegni, N. V. Prokof'ev, and B. V. Svistunov, Superconducting transition temperature of the bose one-component plasma, Phys. Rev. Lett. **130**, 236001 (2023).
- [3] B. K. Chakraverty, J. Ranninger, and D. Feinberg, Experimental and theoretical constraints of bipolaronic superconductivity in high T_c materials: An impossibility, Phys. Rev. Lett. **81**, 433 (1998).
- [4] C. Zhang, J. Sous, D. Reichman, M. Berciu, A. Millis, N. Prokof'ev, and B. Svistunov, Bipolaronic high-temperature superconductivity, Phys. Rev. X **13**, 011010 (2023).
- [5] J. Sous, C. Zhang, M. Berciu, D. Reichman, B. Svistunov, N. Prokof'ev, and A. Millis, Bipolaronic superconductivity out of a coulomb gas, arXiv:2210.14236 (2022).
- [6] S. Ragni, T. Hahn, Z. Zhang, N. Prokof'ev, A. Kuklov, S. Klimin, M. Houtput, B. Svistunov, J. Tempere, N. Nagaosa, C. Franchini, and A. Mishchenko, Polaron with quadratic electron-phonon interaction, Phys. Rev. B **107**, L121109 (2023).
- [7] Z. Zhang, A. Kuklov, N. Prokof'ev, and B. Svistunov, Soliton states from quadratic electron-phonon interaction, Phys. Rev. B **108**, 245127 (2023).
- [8] K. L. Ngai, Two-phonon deformation potential and superconductivity in degenerate semiconductors, Phys. Rev. Lett. **32**, 215 (1974).
- [9] O. Entin-Wohlman, H. Gutfreund, and M. Weger, Mass and frequency renormalization for quadratic electron-phonon coupling, Solid State Communications **46**, 1 (1983).
- [10] P. S. Riseborough, The small polaron with nonlinear electron-phonon interactions, Annals of Physics **153**, 1 (1984).
- [11] O. Entin-Wohlman, H. Gutfreund, and M. Weger, Mass and frequency renormalization for quadratic electron-phonon coupling, Journal of Physics C: Solid State Physics **18**, L61 (1985).
- [12] V. Hizhnyakov, Zero-phonon line: Effect of quadratic electron-phonon coupling, Chem. Phys. Lett. **493**, 191 (2010).
- [13] R. Heid, Relevance of quadratic electron-phonon coupling for the superconducting transition temperature, Phys. Rev. B **45**, 5052 (1992).
- [14] J. A. D. Matthew and A. Hart-Davis, Theory of isotopic effects in the electron-phonon interaction, Phys. Rev. **168**, 936 (1968).
- [15] G. D. Mahan, Reentrant superconductivity from the anharmonic electron-phonon interaction, Phys. Rev. B **56**, 8322 (1997).
- [16] S. Li, E. A. Nowadnick, and S. Johnston, Quasiparticle properties of the nonlinear holstein model at finite doping and temperature, Phys. Rev. B **92**, 064301 (2015).
- [17] D. E. Kiselov and M. V. Feigel'man, Theory of superconductivity due to ngai's mechanism in lightly doped sr₂io₃, Phys. Rev. B **104**, L220506 (2021).
- [18] P. Volkov, P. Chandra, and P. Coleman, Superconductivity from energy fluctuations in dilute quantum critical polar metals, Nat. Comm. **13**, 4599 (2022).
- [19] T. Yildirim, O. Gülseren, J. W. Lynn, C. M. Brown, T. J. Udovic, Q. Huang, N. Rogado, K. A. Regan, M. A. Hayward, J. S. Slusky, T. He, M. K. Haas, P. Khalifah, K. Inumaru, and R. J. Cava, Giant anharmonicity and nonlinear electron-phonon coupling in mgb₂: A combined first-principles calculation and neutron scattering study, Phys. Rev. Lett. **87**, 037001 (2001).
- [20] D. van der Marel, F. Barantani, and C. W. Rischau, Possible mechanism for superconductivity in doped sr₂io₃, Phys. Rev. Res. **1**, 013003 (2019).
- [21] D. Kennes, E. Wilner, D. Reichman, and A. Millis, Transient superconductivity from electronic squeezing of optically pumped phonons, Nat. Phys. **13**, 479 (2017).
- [22] J. Sous, B. Kloss, D. Kennes, D. Reichman, and A. Millis, Phonon-induced disorder in dynamics of optically pumped metals from nonlinear electron-phonon coupling, Nat. Comm. **12**, 5803 (2021).
- [23] V. Esposito, M. Fechner, R. Mankowsky, H. Lemke, M. Chollet, J. M. Glowina, M. Nakamura, M. Kawasaki, Y. Tokura, U. Staub, P. Beaud, and M. Först, Nonlinear electron-phonon coupling in doped manganites, Phys. Rev. Lett. **118**, 247601 (2017).
- [24] M. Schilcher, P. Robinson, D. Abramovitch, L. Tan, A. Rappe, D. Reichman, , and D. Egger, The significance of polarons and dynamic disorder in halide perovskites, ACS Energy Lett. **6**, 2162 (2021).
- [25] A. Kumar, V. I. Yudson, and D. L. Maslov, Quasiparticle and nonquasiparticle transport in doped quantum paraelectrics, Phys. Rev. Lett. **126**, 076601 (2021).
- [26] K. G. Nazaryan and M. V. Feigel'man, Conductivity and

- thermoelectric coefficients of doped SrTiO_3 at high temperatures, *Phys. Rev. B* **104**, 115201 (2021).
- [27] A. Kuklov, Soliton-like excitations in strongly anharmonic media, *Physics Letters A* **139**, 270 (1989).
- [28] A. Gogolin and A. Ioselevich, Quantum polaron, *JETP letters* **53**, 479 (1991).
- [29] A. Gogolin and A. Ioselevich, The effective mass of a quantum polaron, *JETP letters* **54**, 285 (1991).
- [30] C. Adolphs and M. Berciu, Going beyond the linear approximation in describing electron-phonon coupling: Relevance for the holstein model, *Europhys. Lett.* **102**, 47003 (2013).
- [31] A. B. Kuklov, *Superconductivity* **3**, S355 (1990), ISSN 0235-8964 [translation from Russian, *Sverkhprovodimost (KIAE)*, 3 (10), 2277 (1990)].
- [32] Z. Han, S. A. Kivelson, and P. A. Volkov, Quantum bipolaron superconductivity from quadratic electron-phonon coupling, *Phys. Rev. Lett.* **132**, 226001 (2024).
- [33] N. Prokof'ev and B. Svistunov, Phonon-modulated-hopping polarons: X-representation technique, *Phys. Rev. B* **106**, L041117 (2022).